Modeling and Optimization of an Off-Grid Solar- and Wind-Powered Desalination System Integrated with Brine Energy Recovery via Pressure-Retarded Osmosis

Ignacio Schmidhalter[a,1], Miguel C. Mussati[a,2], Mostafa F. Shaaban[b], Pio A. Aguirre[a,3] Tatiana Morosuk[c] and Sergio F. Mussati[a,4]

[a] *Instituto de Desarrollo y Diseño INGAR (CONICET–UTN), Santa Fe, Argentina*
[1] ischmidhalter@santafe-conicet.gov.ar
[2] mmussati@santafe-conicet.gov.ar
[3] paguir@santafe-conicet.gov.ar
[4] mussati@santafe-conicet.gov.ar
[b] *Energy, Water, and Sustainable Environment Research Center, College of Engineering, American University of Sharjah, UAE,* mshaaban@aus.edu
[c] *Institute for Energy Engineering, Technische Universität Berlin, Germany,* tetyana.morozyuk@tu-berlin.de

Abstract:

Autonomous (off-grid) desalination powered by renewable energy is a key solution for ensuring a sustainable water supply in remote and isolated regions. However, brine discharge remains a major environmental concern, as high-salinity effluents can adversely affect marine ecosystems by altering local salinity levels and impacting biodiversity.

This work addresses the design and optimization of an integrated off-grid desalination system operating under a Zero Brine Discharge (ZBD) strategy. The proposed system combines multiple desalination and energy recovery technologies, including reverse osmosis, electrodialysis, pressure retarded osmosis, and crystallization, only powered by solar and wind energy. In this study, ZBD is defined as achieving a final effluent salinity comparable to seawater by controlled integration of low-salinity wastewater streams, thereby mitigating environmental impacts.

A mixed-integer linear programming model is developed to identify the optimal system configuration from a superstructure embedding multiple feasible alternatives, while simultaneously determining equipment sizing and operating conditions. The model is implemented within an hourly optimization framework (8760 h), accounting for renewable energy intermittency using representative meteorological year data and time-varying water demand.

The mixing of low-salinity wastewater with a fraction of RO brine is identified as the most cost-effective configuration, resulting in the largest reduction in water production costs. When potential revenues from salt recovery are included, the economic advantage persists but is less pronounced. Depending on the process configuration, results indicate that the levelized cost of water ranges from 1.87 to 2.5 USD/m³, and when salt is considered a valuable by-product, the cost decreases to 0.60 – 1.62 USD/m³.

This work provides a comprehensive framework for the design of self-sufficient and environmentally sustainable desalination systems, highlighting the potential of brine valorization and the integration of alternative water sources.

Keywords:

Zero Brine Discharge (ZBD); Green Desalination; Optimisation; Sustainability.

1. Introduction

Although several studies have addressed ZBD systems, none have systematically investigated the full range of possible configurations arising from the integration of RO, ED, and PRO technologies and different streams mixing. Moreover, previous works have not considered the simultaneous optimization of process configuration, energy integration, and water management strategies within a unified framework. As a result, the problem becomes highly combinatorial.

2. Process description

Figure 1 presents an alternative configuration for an off-grid desalination process operating under a ZBD criterion. As shown, raw seawater (RSW) is first pumped to a buffer tank (Tk_{RSW}) via pump P_RSW. It is then pressurized and fed to the reverse osmosis (RO) unit, producing a permeate stream (freshwater, W_{RO}) and a retentate stream (concentrated brine, B_{RO}). The brine stream is directed to a brine storage tank (Tk_{BRO}) and subsequently treated in the electrodialysis (ED) unit. The ED unit generates a treated water stream (WED) with salinity comparable to that of seawater, enabling environmentally compliant discharge, and a more concentrated brine stream, which is sent to the brine buffer tank (Tk_{BED}). The concentrated brine from Tk_{BED} is then fed to a crystallization unit (CRY), where solid salt (SALT) is recovered, thereby reducing liquid discharge. CRY primarily involves mechanical vapor-compression stages. Meanwhile, freshwater produced by the RO and CRY units is stored in the freshwater tank (Tk_{FW}) to meet the freshwater demand (W_{DEM}). The overall process is powered by renewable solar and wind energy sources and incorporates a battery energy storage system (BESS) to manage their intermittency. Any excess energy that cannot be utilized or stored is curtailed (E^{CURT}).

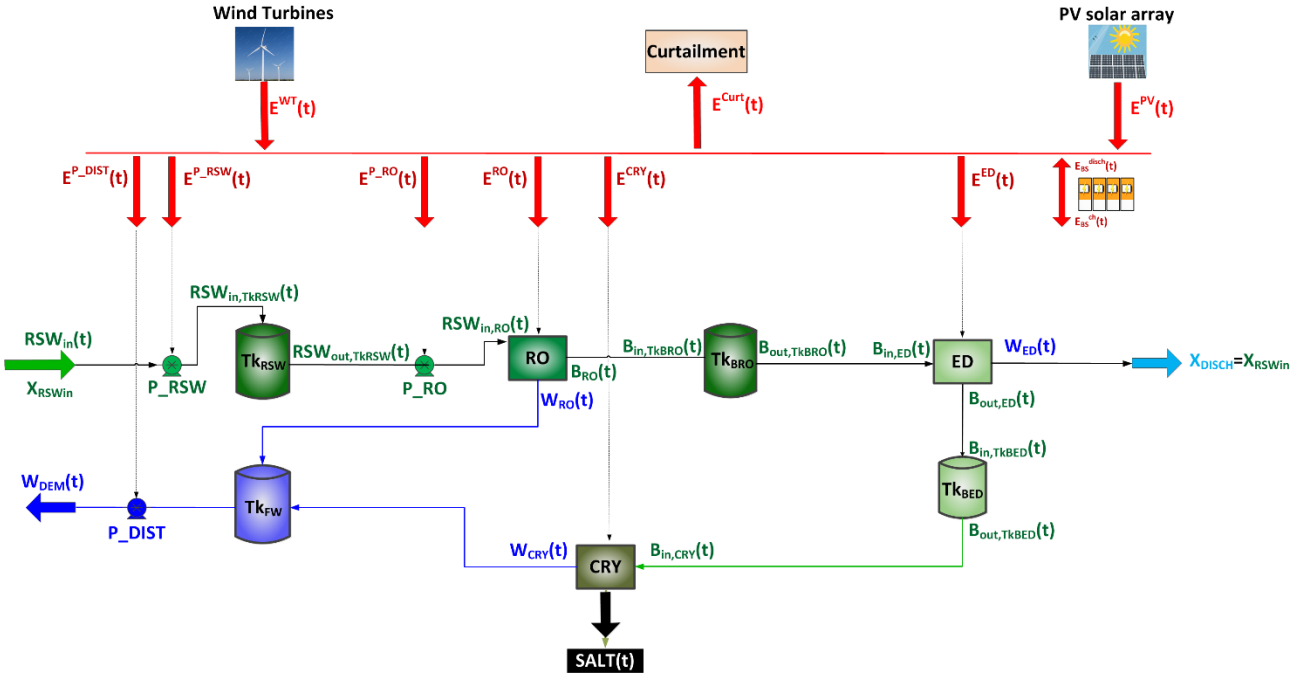

***Figure 1**. Conventional off-grid ZBD desalination system (Alternative 1, lowest level of process integration).*

3. Optimal design problem statement

Starting from the configuration described in Fig. 1, corresponding to the baseline (simplest) alternative, a superstructure-based representation is proposed (Fig. 2) that embeds multiple alternative configurations from which the optimal solution is systematically determined. To this end, five splitters (SPL-1 to SPL-5) and two mixers (MX-1 and MX-2) are strategically incorporated into the baseline configuration to enable different flow patterns and, consequently, a wide range of process configurations.

In addition, a Pressure Retarded Osmosis (PRO) unit is included in the superstructure to exploit the salinity gradient between the concentrated RO brine and a low-salinity stream for power generation. Furthermore, the possibility of utilizing low-salinity wastewater from the served population to dilute the brine, when beneficial, is incorporated through the wastewater tank (Tk_{WW}).

In the proposed superstructure (Figure 2), the units RO, ED, CRY, Tk_{BED}, Tk_{RSW}, Tk_{BRO} and Tk_{FW}, as well as the streams represented by solid lines, are always present in the model. In contrast, the mixers (MX-1 and MX-2) and splitters (SPL-1 to SPL-5) are optional and may be either included or removed, allowing the model to represent a broad set of alternative configurations within a unified framework. For instance, if SPL-2 is not included, the PRO unit cannot be activated. When splitter SPL-2 operates with full flexibility, the brine leaving the brine buffer tank of ED (Tk_{BED}) can be distributed among multiple pathways: (1) a fraction could be directed to the PRO unit for energy recovery; (2) another fraction could be sent to the crystallization unit (CRY); and (3) another portion could be mixed with wastewater from Tk_{WW} to achieve the discharge concentration of 50 g/l.

The model is formulated so that process units can be effectively deactivated when the associated flow variables—particularly those linked to splitters—are zero, without the need to introduce binary variables. This feature is advantageous, as it avoids increasing model complexity and facilitates numerical solutions.

Table 1 summarizes several alternative configurations embedded in the superstructure, arising from different feasible combinations of Reverse Osmosis (RO), Electrodialysis (ED), Pressure Retarded Osmosis (PRO), and crystallization (CRY) units. In Table 1, the symbol "✓" indicates that the given possibility is available for inclusion; however, it does not guarantee its inclusion in the optimal solution. For example, if PRO is marked with "✓," this means that it can be included by activating the corresponding splitter (SPL-2) and therefore represents a decision variable within the model. In contrast, the symbol "X" indicates that the given possibility is not available and cannot be part of the optimal solution under any circumstances.

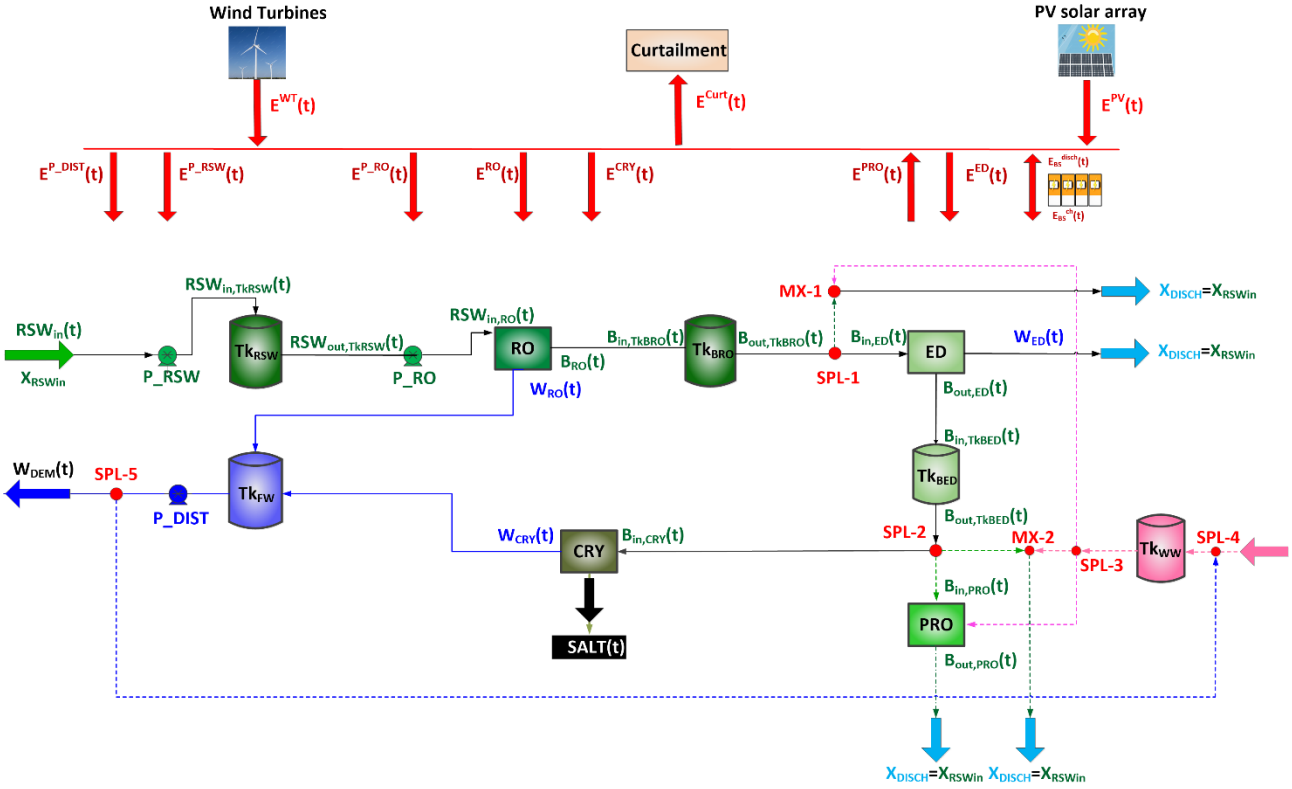

Figure 2. *Superstructure-based representation encompassing multiple alternative configurations derived from Fig. 1 (Alternative #2, most comprehensive configuration).*

Table 1. *Representative alternatives embedded in the proposed superstructure in Fig. 2.*

Alternative	PRO	Mix BED (MBED)	Mix WW (MWW)	Mix FW (MFW)	Mix BRO (MBRO)
#1 (baseline)	X	X	X	X	X
#2 (full superstructure)	✓	✓	✓	✓	✓
#3	X	✓	✓	X	X
#4	X	✓	X	✓	X
#5	✓	X	✓	X	X
#6	✓	✓	✓	X	X
#7	X	✓	✓	✓	X
#8	✓	X	X	✓	X
#9	✓	✓	X	✓	X
#10	✓	X	✓	✓	X
#11	✓	✓	✓	✓	X
#12	X	X	✓	X	✓
#13	✓	X	✓	X	✓
#14	✓	X	X	✓	✓

Note: ✓ indicates that the unit or option is available for inclusion in the optimization model, while X indicates that it is excluded.

As shown in Table 1, the investigated configurations differ not only in the selected desalination technologies but also in how low-salinity wastewater and freshwater streams are utilized. Specifically, these streams may be (i) mixed with brines from desalination units (RO or ED) to satisfy discharge salinity constraints, or (ii) used as diluted feed in PRO systems for energy recovery.

The system is constrained to meet the hourly water demand variable along the year while ensuring that the final discharge reaches seawater salinity, thereby avoiding adverse environmental impacts associated with brine disposal.

The optimization problem is formulated as a mixed-integer linear programming (MILP) model that determines the optimal process configuration, equipment sizing, and operating conditions to minimize the levelized water cost. The model includes mass and energy balance equations for all process units, as well as capacity constraints and operational limits. The ZBD condition is enforced through salinity constraints on the final discharge streams. Continuous variables describe mass and energy flows, salinity levels, and storage dynamics, while binary variables represent the operating status of the RO unit.

The optimization is carried out over an hourly time horizon (8760 h), allowing for the explicit representation of renewable energy intermittency and time-varying water demand. Energy storage is incorporated through a battery energy storage system (BESS). Ensuring an exact hourly balance among energy generation, storage dynamics, tank inventories, and freshwater production is challenging due to the inherent trade-offs in the optimization problem.

The objective function minimizes the total annual cost (capital investment and operating and maintenance costs).

4. Mathematical model

For the model implementation, a set T containing 8760 elements 't' is defined to account for the variations of the main optimization variables with time. Thus, an element 't' represents a time period of one hour.
The overall energy balance is imposed at each time period 't' (1 hour), ensuring that total energy supply equals total energy demand and that storage interactions are accounted for.

$$E^{PV}(t)+E^{WT}(t)+E^{BESS}_{disch}(t)+E^{PRO}(t)=E^{CURT}(t)+E^{BESS}_{ch}(t)+E^{RO}(t)+E^{ED}(t) \\ +E^{CRY}(t)+E^{P\_RSW}(t)+E^{P\_RSW}(t)+E^{P\_RO}(t)+E^{P\_TkFW}(t)+E^{P\_DIST}(t) \qquad t=1,2...T \qquad (1)$$

where *E(t)* (kWh) represents the energy exchanged during time interval *t*, and the superscripts indicate the subsystem under consideration.

To illustrate the mass and energy balances considered for the process units, the RO unit is used as a representative, expressed from Eq. (2) to (5).

$$RSW^{TkRSW}_{out}(t)=RSW^{RO}_{in}(t) \qquad t=1,2...T \qquad (2)$$

$$RSW^{RO}_{in}(t)=W^{RO}(t)+B^{RO}(t) \qquad t=1,2...T \qquad (3)$$

$$B^{RO}(t)=W^{RO}(t)\,\frac{1-RR_{RO}}{RR_{RO}} \qquad t=1,2...T \qquad (4)$$

$$E^{RO}(t)=W^{RO}(t)\,SEC^{RO} \qquad t=1,2...T \qquad (5)$$

- Logical constraints for unit operation

The on/off operation of the RO unit is modeled through the following constraint:

$$E^{RO}(t)\le M_{RO}\,y(t) \qquad t=1,2...T \qquad (6)$$

where *y(t)* is a binary variable equal to 1 when the RO unit is operating and 0 otherwise. M_{RO} represents the big-M values usually four or five times higher than $E_{RO}(t)$.

Equation (7) enforces a minimum flexibility value ($FLEX^{RO}$ = 40%) when the unit is active (y(t)=1):

$$P^{RO}_N\,FLEX^{RO}\le E^{RO}(t)/\Delta t+M_{RO}(1-y(t)) \qquad t=1,2...T \qquad (7)$$

- Ramp-up and ramp-down constraints

The dynamic operation of the RO unit is further constrained through ramping limits:

$$(E^{RO}(t+1)-E^{RO}(t))/\Delta t\le 0.10\,P^{RO}_N+M_{RO}(1-y(t)+1-y(t+1)) \qquad t=1,2...T-1 \qquad (8)$$

$$(E^{RO}(t)-E^{RO}(t+1))/\Delta t\le 0.16\,P^{RO}_N+M_{RO}(1-y(t)+1-y(t+1)) \qquad t=1,2...T-1 \qquad (9)$$

These constraints limit the rate of change in power consumption between consecutive time periods, ensuring realistic operational transitions.

Equivalent mass balances, energy balances, and operational constraints to those in Eqs. (1)–(8) are defined for the ED, CRY, and PRO units.

With regards to inventory levels (I) of buffer tanks, Eq. (9) illustrates the balance for the brine buffer tank associated with the RO unit. Equivalent balances are proposed for the remaining tanks (Tk_{RSW}, Tk_{FW}, Tk_{BED}, Tk_{WW}).

$$I^{Tk_{BRO}}(t+1) = I^{Tk_{BRO}}(t) + (B^{RO}(t) - B_{in}^{ED}(t))\,\Delta t \qquad t = 1,2...T-1 \tag{10}$$

- Objective Function

The objective is to minimize the levelized cost of water (LCOW), including capital investment, operation and maintenance, and energy-related costs:

$$LCOW = \frac{\sum_j (CAPEX(j)\ CRF + OPEX(j))}{\sum_t W_{DEM}(t)} \tag{11}$$

where the subscript *j* refers to each process unit. The parameter CRF denotes the capital recovery factor, calculated under a 3% discount rate and a 20-year project lifetime.

5. Results

By solving the proposed superstructure-based model, the optimal configuration was identified as the most comprehensive alternative listed in Table 1 (Alternative #2), achieving the minimum levelized cost of water (LCOW) of 1.88 $/m³. The corresponding optimal design includes nominal power of 4328 kW for the solar farm and 193 kW for the wind farm, along with a battery energy storage system (BESS) rated at 1592 kW of peak power and 7962 kWh of capacity.

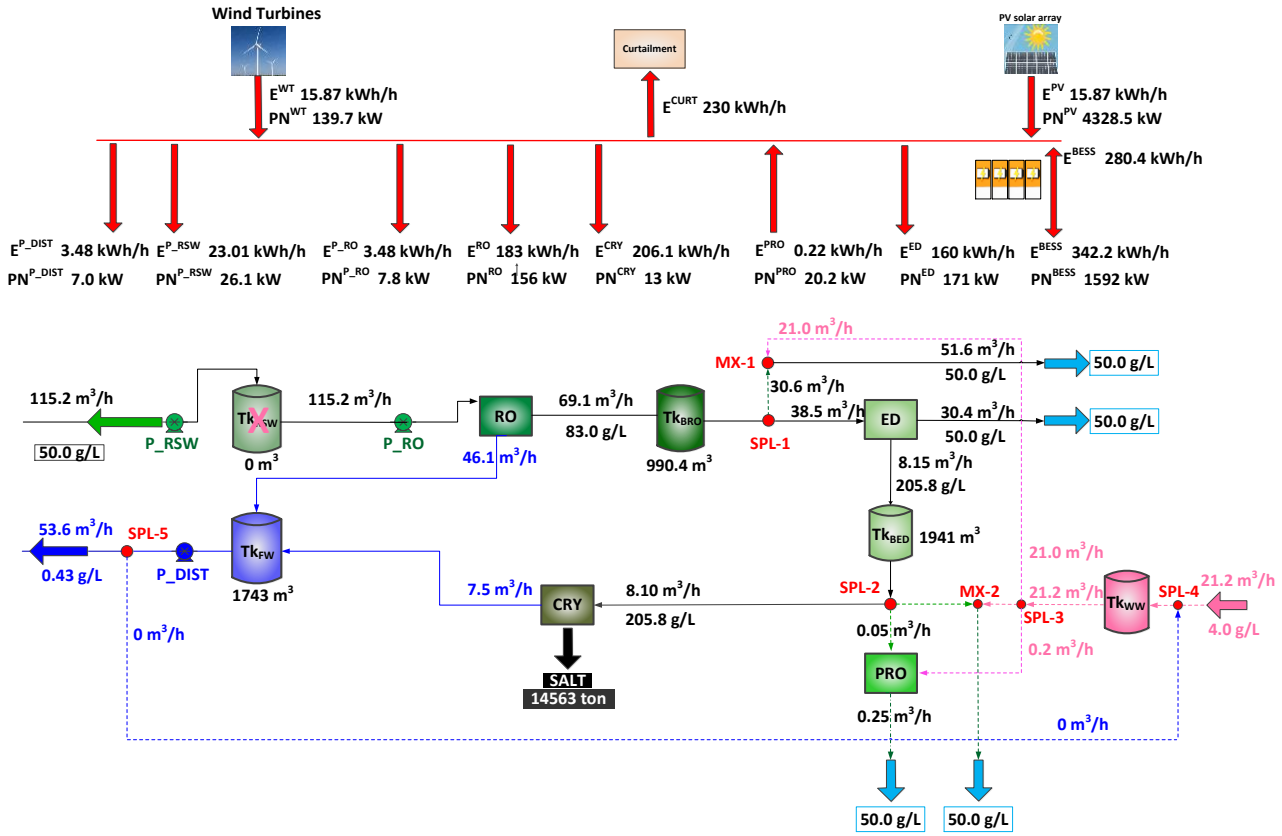

Figure 3*. Optimal system configuration, including process unit sizing and annual average values of flow rates and energy-related variables.*

The Tk_{RSW} tank is not selected in the optimal solution. Wastewater is used to mix with the brine streams leaving both the RO and ED buffer tanks, as illustrated in Fig. 3. As assumed in the model, the ZBD implies that the concentrations of the streams discharged to the sea are equal to the inlet seawater concentration (50 g/L).

For illustrative purposes and to ensure completeness of the presentation, Fig. 3 shows the flow rates and concentrations of all streams, as well as the sizing of each selected process unit. This includes the power consumption of RO, ED, and CRY; the storage capacities of the brine and freshwater buffer tanks; and the installed capacities of the solar and wind systems, along with the curtailed energy, battery storage capacity and the contribution of PRO in generating electricity. It is important to note that the reported flow rates correspond to annual average values. Therefore, although some of these average values may appear low, they are not necessarily representative of specific time periods, during which they may double or even triple. For example, although the reported annual average flow rate for the inlet stream of the PRO unit is 0.05 m^3/yr, during the time interval between hours 1627 and 1663, the flow rate reaches approximately 5.4 m^3/h. A similar situation is observed for PV generation: while the annual average value is 814.3 kWh/h, it can reach up to 4328.5 kWh/h in several moments during the year, for example, at hour 3133.

Figure 4 presents the LCOW (red) calculated without considering salt sales; LCOW-S (blue), including revenues from salt; and the total plant power (green) for all alternatives listed in Table 1. Plant power involves all the process units that require energy.

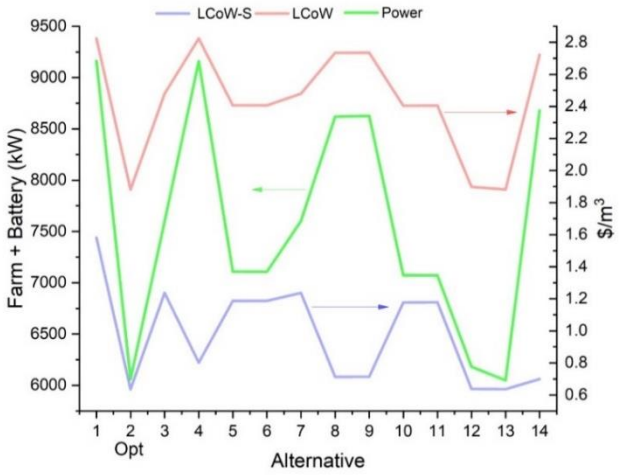

Figure 4. *Optimal LCOW (excluding salt sales), LCOW-S (including salt sales), and total plant power corresponding to each alternative configuration in Table 1.*

As shown, the LCOW values across the alternative configurations range from 1.88 to 2.80 \$/m^3. When salt sales revenues are considered, the LCOW decreases, yielding the LCOW-S values. In this context, salt production varies significantly among the alternatives, and LCOW-S is calculated assuming a selling price of 40 \$/t. Salt production emerges as a key variable that should be explicitly accounted for in the analysis. Indeed, when this factor is included, the cost of water can be substantially reduced, potentially leading to a shift in the optimal design toward different configurations. The optimization of the overall process based on a profit-driven objective function is beyond the scope of this work and is left for future research.

Figures 5 and 6 present the nominal (peak) power of the main system components for each alternative configuration in separate and stacked forms, respectively, providing insight into the design trade-offs underlying the LCOW results shown in Figure 4. Overall, the results in Figures 4–6 indicate that configurations with higher installed capacities of solar generation and BESS tend to exhibit lower LCOW values, as they enhance renewable energy availability and reduce reliance on unmet demand or inefficient operation. The solar park dominates the energy supply across all alternatives, while the contribution of wind energy remains comparatively limited (Figs. 5 and 6). The BESS plays a key role not only in mitigating intermittency but also in ensuring the technical and operational feasibility required to guarantee the continuous operation of the CRY unit. with larger storage capacities generally associated with improved system performance and lower water production costs. However, increasing installed capacity also entails higher capital expenditures, leading to a trade-off between investment costs and operational efficiency, which explains the variability in LCOW across the alternatives in Fig. 4.

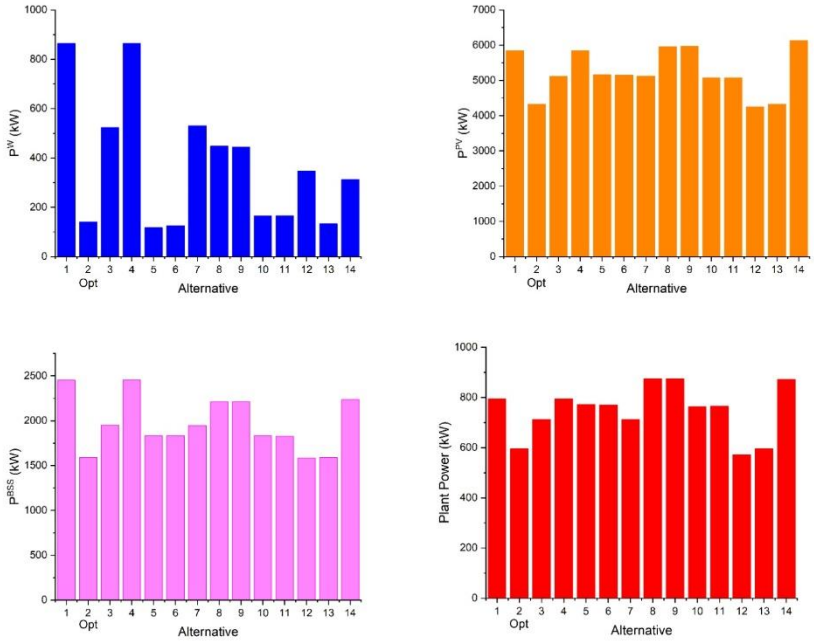

Figure 5. *Nominal capacities of wind and solar power farms, nominal peak power of the BESS, and total plant power demand (including pumps and the RO unit).*

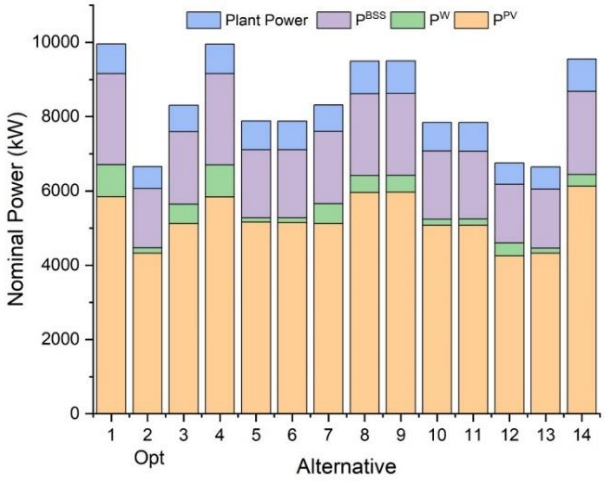

Figure 6. *Comparison of optimal nominal power capacities for the overall plant, BESS, and solar and wind farms across the alternative configurations in Table 1, shown in stacked form.*

Figure 7 illustrates the distribution of nominal (peak) power among the individual desalination units for each alternative. Electrodialysis (ED) and the crystallization system—comprising mechanical vapor compression (MVC) and the crystallizer (CRY)—clearly dominate the overall power demand, jointly accounting for the largest share of total peak power (typically around 60–75%). Reverse osmosis (RO) represents a secondary yet significant contribution, accounting for approximately 15–25% of the total. In contrast, pressure retarded osmosis (PRO), which operates as an energy recovery unit, has a marginal impact on the overall power contribution, generally contributing less than 5%.

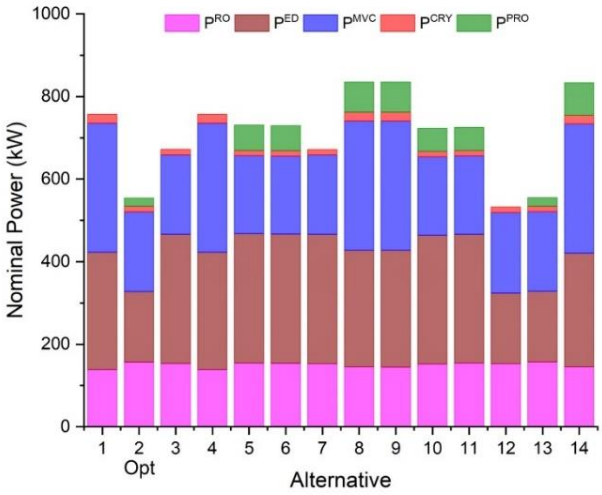

Figure 7. *Comparison of optimal nominal power capacities of individual desalination units across the alternative configurations in Table 1, shown in stacked form.*

Temporal Behavior of Flow Rates and Storage Inventories.

To illustrate the optimal performance of the integrated ZBD system under Alternative #2, a representative subset of hourly results is extracted from the full annual solution (8760 hours). The selected time window (hours 950–1050) captures the key operating dynamics of renewable generation, battery cycling, and process interactions. The results are presented in the following order: Fig. 8 shows the energy generation and storage behavior; Fig. 9 illustrates the evolution of tank inventory levels; Fig. 10 presents the power consumption of each unit; Fig. 11 shows the discharge flows and salt production; Fig. 12 reports the internal flow rates; and Fig. 13 provides the detailed hourly energy allocation, including curtailment. It should be noted that the energy values reported (e.g., in Figs 10, 11, and 13) correspond to the energy exchanged over each 1-hour time interval (Δt = 1 h). Accordingly, the average power is obtained as E(t)/Δt (kW).

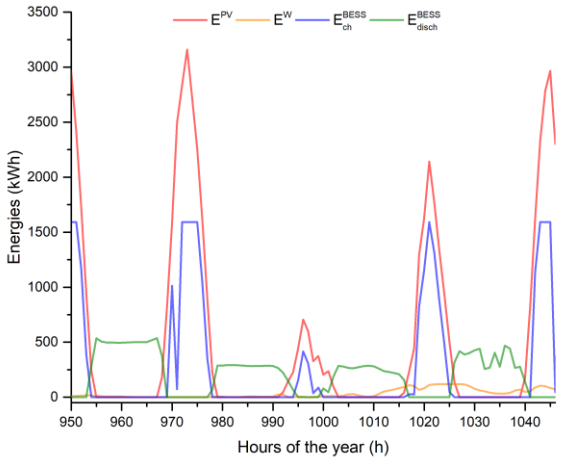

Figure 8. *Optimal profiles of renewable energy generation and battery charging/discharging over the hourly time horizon.*

Figure 8 shows that, during the earlier period (h 950–965), PV generation rapidly decreases from high values to zero at hour 955, marking a transition from high to low renewable availability. During this interval, the battery shifts from charging to discharging mode, supplying energy to compensate for the reduction in solar output and maintain the supply–demand balance. Subsequently, during central daylight hours (e.g., h 967–980, 995–1000 and 1016–1026), surplus PV generation drives battery charging (E^{BESS}_{ch}), with values reaching up to 1590 kWh. Conversely, then during nighttime and low-irradiation periods (e.g., h 1030–1050), the battery discharges (E^{BESS}_{disch}) to supply energy to the desalination units and meet demand. Wind power provides a continuous but relatively low baseline contribution. Overall, the charge/discharge pattern shown in Figure 8 is essential for Alternative #2 to decouple renewable generation from demand, thereby ensuring continuous

water production without an external electricity supply and contributing to achieving the minimum levelized cost of water (LCOW).

Figure 9 shows the evolution of storage tank levels. The Tk_{FW} exhibits a highly dynamic and cyclic behavior, characterized by frequent charging and depletion phases, with sharp increases and decreases in inventory levels. This reflects the direct coupling between freshwater production and time-varying demand. In contrast, Tk_{BED} shows a much smoother and more gradual trend, with a predominantly monotonic increase over extended periods and significantly lower short-term variability. The wastewater tank (Tk_{WW}) fluctuates within a relatively narrow range, between 0 and 180 m³, indicating a more limited but controlled buffering role.

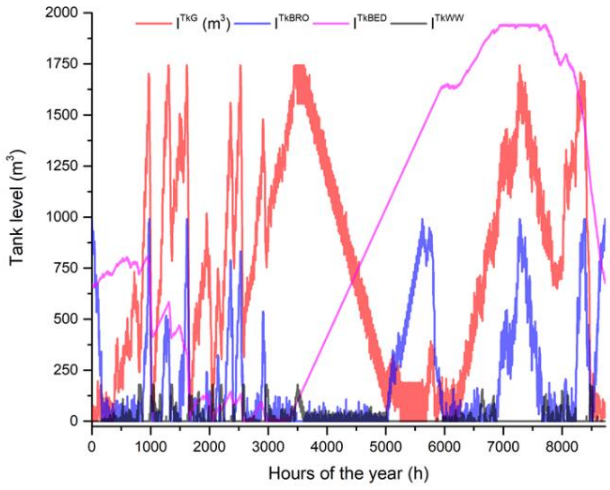

***Figure 9**. Temporal evolution of optimal inventory levels in freshwater, brine, and wastewater storage tanks.*

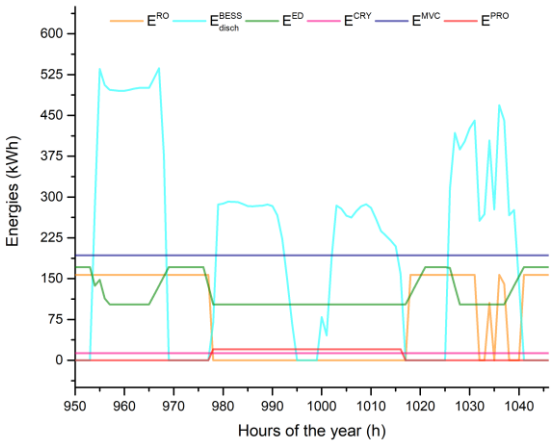

***Figure 10.** Optimal energy consumption profiles of desalination units and battery discharge over hourly time periods.*

Figure 10 presents the hourly energy consumption of each process. The RO unit operates intermittently, with alternating active and inactive periods, while offering operational flexibility when active. Electrodialysis operates within a range of approximately 103–171 kWh. In the crystallization process the MVC and CRY units operate at constant levels of 193 kWh and 13 kWh, respectively. The PRO unit is fully flexible and operates intermittently, with peak values of around 25–30 kWh. Battery discharge energy (E^{BESS}_{disch}) shows the highest fluctuation, ranging from 0 up to approx. 530 kWh, highlighting its key role in balancing energy supply and demand.

Figure 11 reports the discharge streams, including the diluted ED stream (W_{ED}), the blended RO brine stream (W_{MBRO}), and the permeate stream from the PRO unit ($W_{out,PRO}$), all satisfying the ZBD condition (50 g/L salinity). It can be observed that the PRO unit does not operate continuously, as it remains inactive during the

period h 980–1015. A similar trend is observed between W_{ED} and W_{MBRO}, suggesting coordinated operation to meet discharge constraints. In addition, salt is continuously produced at a constant rate of 1667 kg/h.

Figure 12 shows the optimal temporal evolution of total freshwater production, including the contributions from RO and CRY, together with the inventory level of the freshwater tank (Tk_G=Tk_{FW}). It can be observed that, during the period h 950–955, water demand is satisfied by the combined production of RO and CRY, as the inventory level (I^{TkFW}) remains approximately constant. Between hours 955 and 970, water demand decreases, while RO continues operating at its maximum capacity, leading to an increase in the tank inventory. During the interval h 980–1017, water demand is met by the contribution of CRY and the withdrawal from the freshwater tank, as the RO unit is not operating. In contrast, between hours 1017 and 1032, water demand is satisfied by both CRY and RO production, with RO operating continuously at maximum capacity, resulting in a nearly constant inventory level. Finally, during the time period 1032–1050, demand is covered by CRY production, intermittent operation of RO, and withdrawals from the freshwater tank. Crystallizer water production (W_{CRY}) remains constant at 7.5 m³/h throughout the entire time horizon, indicating a lack of operational flexibility.

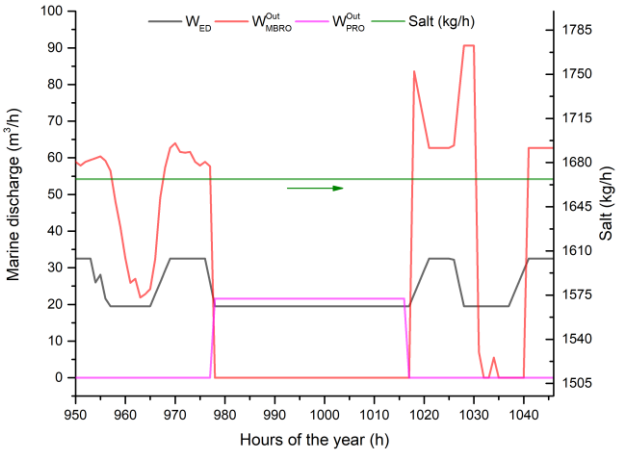

***Figure 11**. Discharge streams satisfying the ZBD condition (50 g/L): diluted ED stream (W_{ED}), blended RO brine ($W_{out,MBRO}$), and PRO permeate ($W_{out,PRO}$).*

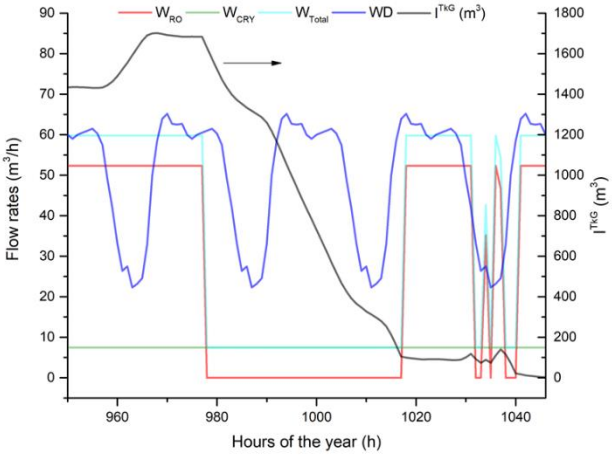

***Figure 12**. Optimal temporal evolution of freshwater production from the different desalination units (RO, ED, and CRY) contributing to the satisfaction of the water demand*.

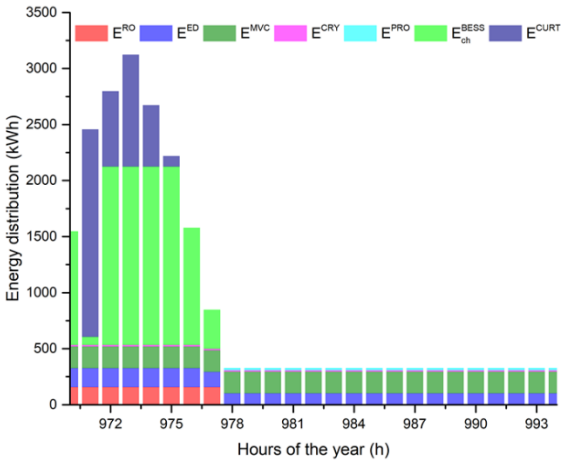

***Figure 13**. Optimal energy allocation among desalination processes, battery energy storage system (BESS), and curtailment over hourly time periods*.

igure 13 provides a detailed hourly breakdown of electricity allocation among all processes, battery charging, and curtailment. In contrast to other time periods, during high electricity-generation intervals (e.g., h 971–977), the available energy is primarily allocated to battery charging (up to approximately 1500 kWh) and RO operation. Despite this, a non-negligible amount of energy is curtailed (E^{CURT}). This indicates that, from the perspective of the objective function (cost minimization), further utilization of the excess energy is not economically justified, leading to its curtailment.

6. Conclusions

This study developed a mixed-integer linear programming (MILP) framework to optimize the configuration, sizing, and operation of an integrated desalination and energy system. The main findings are summarized as follows:

- In the optimized configuration (Fig. 3), although the use of freshwater for brine dilution is allowed, only wastewater is utilized. In this case, wastewater is used to dilute brine streams from the RO and ED units and to feed the PRO unit, thereby reducing the required capacity of downstream units and, consequently, the overall system cost.
- The integration of Pressure Retarded Osmosis (PRO) is consistently selected when available. Its contribution is primarily the reduction of battery energy storage requirements; however, its power generation potential is limited by the availability of low-salinity wastewater. The relatively high capital cost assumed for PRO suggests that further cost refinement is needed.
- The mixing of low-salinity wastewater with RO brine is systematically identified as the most cost-effective configuration, leading to the largest reduction in water production cost. When potential revenues from salt recovery are included, the economic advantage persists but is less pronounced.
- The mixing of electrodialysis (ED) brine with wastewater is only optimal in a subset of cases (Alternatives 2, 3, 6, 7). In other feasible cases (e.g., Alternatives 4, 9), the model does not select this option, indicating a limited economic benefit under the studied conditions.
- The results presented motivate further research, including the development of a more detailed cost model and the evaluation of different seawater concentrations.

Nomenclature

$\dot{B}$	mass flow rate of brine, m^3/h
$CAPEX$	capital expenditure, \$
E	energy, kWh
ED	electrodialisis
I	inventory levels in tanks, m^3
$LCOW$	levelised water cost, $/m^3$
M_{RO}	big-M value

$OPEX$ operating expenditure, $/yr
P_RSW raw sea water pump
P_RO reverse osmosis pump
P_DIST water distribution pump
P_N nominal power, kW
RO reverse osmosis
$\dot{RSW}$ mass flow rate of raw sea water, m^3/h
SEC specific energy consumption (kWh/m^3)
TAC total annual cost, $/yr
$\dot{W}$ mass flow rate of freshwater, m^3/h
$\dot{W}_{DEM}$ fresh water demand, m^3/h
$y_{(t)}$ binary variable, dimensionless

Subscripts and superscripts

BED brine coming from ED
BRO brine coming from RO
$CURT$ curtailment
ED electrodialisis
j process unit
PV photovoltaic system
PRO pressure retarded osmosis
RO reverse osmosis
t hour
Tk tank
WT wind farm

References

[1] Abobeh S., Abdelsalam M.M., Bouz, M.A.E, An Overview Study on Water Desalination, Hybrid RO Systems, and How to Utilize Artificial Intelligence with the System. Water Conserv Sci Eng 2025; 10: 85. https://doi.org/10.1007/s41101-025-00409-5